# Long-term hepatotoxicity of polyethylene-glycol functionalized multi-walled carbon nanotubes in mice

To cite this article: Danying Zhang *et al* 2010 *Nanotechnology* **21** 175101

Nanotechnology **21** (2010) 175101 (10pp) doi:10.1088/0957-4484/21/17/175101

# Long-term hepatotoxicity of polyethylene-glycol functionalized multi-walled carbon nanotubes in mice

**Danying Zhang[1,3], Xiaoyong Deng[2,3], Zongfei Ji[1], Xizhong Shen[1], Ling Dong[1,4], Minghong Wu[2,4], Taoying Gu[1] and Yuanfang Liu[2]**

[1] Department of Gastroenterology, Zhongshan Hospital, Fudan University, Shanghai 200032, People's Republic of China
[2] Institute of Nanochemistry and Nanobiology, Shanghai University, Shanghai 200444, People's Republic of China

E-mail: dltalk@tom.com and mhwu@staff.shu.edu.cn

Received 10 December 2009, in final form 2 March 2010
Published 1 April 2010
Online at stacks.iop.org/Nano/21/175101

**Abstract**
The toxicity of polyethylene-glycol functionalized (PEGylated) multi-walled carbon nanotubes (MWCNTs) and non-PEGylated MWCNTs *in vivo* was evaluated and compared. Mice were exposed to MWCNTs by intravenous injection. The activity level of glutathione, superoxide dismutase and gene expression in liver, as well as some biochemical parameters and the tumor necrosis factor alpha level in blood were measured over 2 months. The pathological and electron micrographic observations of liver evidently indicate that the damage caused by non-PEGylated MWCNTs is slightly more severe than that of PEGylated MWCNTs, which means that PEGylation can partly, but not substantially, improve the *in vivo* biocompatibility of MWCNTs.

## 1. Introduction

Motivated by various novel properties of carbon nanotubes (CNTs), research into CNTs for biomedical applications has been progressing rapidly in the past few years. A CNT-based nanoplatform has been developed to shuttle various biological molecular cargoes into cells, including drugs, peptides, proteins, plasmid DNA, and small interfering RNA. In addition, CNTs can be used in various biological imaging techniques and cancer therapeutics [1].

For those biomedical applications, surface chemical modification or functionalization is usually required to solubilize CNTs and to give better biocompatibility and low toxicity. Various covalent and noncovalent reactions have been developed to functionalize CNTs. Many types of organic molecule, biomolecule or polymer were used to solubilize CNTs in water, such as hydrophilic molecules, lipids, sugars, proteins, DNA, and polymers [2]. Among these functional groups, polyethylene glycol (PEG) is one of the most promising conjugates for functionalizing CNTs. The PEG functionalized (PEGylated) CNTs are not only highly water soluble but also highly stable in various biological solutions including serum [3]. Furthermore, PEGylation enables CNTs to have a long blood circulation and low uptake in the reticuloendothelial system *in vivo*, which is one of the most important issues for the potential clinical applications of nanomaterials [4]. In recent years, several groups have reported some exciting cases of the bio-applications of PEGylated CNTs. Dai and his colleagues have succeeded in using PEGylated single-walled CNTs (SWCNTs) for a range of biomedical applications including biological sensing, imaging and cancer treatment *in vitro* with cells or *in vivo* with animals [2]. Cato *et al* [5] and Ou *et al* [6] have shown that functional SWCNTs based on an integrin alpha(v)beta(3) monoclonal antibody presented a high targeting efficiency toward cancer cells. In 2008, Cheng *et al* reported that PEGylated SWCNTs could reversibly accumulate in the nucleus of several mammalian cell lines and did not cause discernible changes in the nuclear organization [7]. These observations suggest PEGylated CNTs might be used as an ideal nanovector in biomedical and pharmaceutical applications.

[3] D Y Zhang and X Y Deng contributed equally to this work.
[4] Author to whom any correspondence should be addressed.

 

However, the safety of the nanomaterials has been a serious concern, and must be established as a prerequisite before introduction into the body. A large number of *in vivo* tests have reported that raw CNTs show obvious pulmonary toxicity including unusual inflammation and fibrotic reactions [8]. A pilot study on long CNTs intraperitoneally injected into mice showed asbestos like pathogenic behaviors [9]. These important findings have suggested potential adverse effects of CNTs on human health, but they have not clarified whether and how the chemical functionalization influences the toxicity of CNTs. In fact, many studies have preliminarily shown that physical and chemical parameters, such as length, impurities and surface functionalization of CNTs, do influence their toxicity and biocompatibility [10]. Thus, for the sake of future biomedical applications, it is necessary to fully address the toxicology of the widely recognized PEGylated CNTs, particularly in comparison with that of the non-PEGylated CNTs. Fortunately, a host of existing *in vitro* tests have shown that PEGylated CNTs exhibit neither enhanced apoptosis/neurosis nor reduced proliferation of various cell lines [11–13]. But, as to the *in vivo* toxicity of PEGylated CNTs, related studies are quite limited [14, 15]. Only one paper has reported there was no evident toxicity of PEGylated SWCNTs within 4 months after being injected into the bloodstream of mice. However, we suggest that this result of the low toxicity of PEGylated SWCNTs needs to be repeated because only a few mice (three) were tested in that experiment [15].

In this paper, we intensively investigate the *in vivo* toxicity of PEGylated multi-walled CNTs (P-MWCNTs). As a comparison, the toxicity study of non-PEGylated MWCNTs (NP-MWCNTs) was also studied. Some important toxicological data, such as aspartate aminotransferase (AST), alanine aminotransferase (ALT), creatinine (Cr), total bilirubin (TB), and tumor necrosis factor alpha (TNF-$\alpha$) levels in blood as well as oxidative stress and gene expression are presented. In addition, histopathological observation and transmission electron microscopy (TEM) examination of liver exposed to different doses of P-MWCNTs or NP-MWCNTs were also conducted.

## 2. Materials and methods

### *2.1. Materials*

Pristine MWCNTs (diameter 10–20 nm, length 5–50 $\mu$m, purity >95 wt%) produced by chemical vapor deposition were purchased from Shenzhen Nanoharbor, China. Diamine-terminated PEG ($M_w$ = 1500) was purchased from Sigma-Aldrich (USA). Glutathione (GSH) and superoxide dismutase (SOD) detection kits were purchased from Nanjing Jiancheng Bioengineering Institute (Jiangsu Province, China). All other chemicals, purchased from Sinopharm Chemical Reagent Company, China, were of analytical grade and used without further purification.

### *2.2. Preparation and characterization of P-MWCNTs and NP-MWCNTs*

Prior to preparing P-MWCNTs and NP-MWCNTs, the acid-treated MWCNTs were prepared according to the following procedure. In brief, 500 mg of pristine MWCNTs were dispersed in 300 ml of a 3:1 (V/V) mixture of $H_2SO_4$ and $HNO_3$. After ultrasonication at 40 °C for 7 h, the mixture was diluted with ice water and filtrated with cellulose membrane (pore size = 0.22 $\mu$m), and washed with deionized water several times until the pH of filtrate was about 7. Finally, the black product was collected and dried in a vacuum oven at 40 °C for 24 h.

Then P-MWCNTs were prepared and characterized as described in our previous work [16]. Briefly, 30 mg dried, acid-treated MWCNTs were suspended in 3 ml thionyl chloride with 5 ml additional dimethyl formamide, and the suspension was stirred and refluxed (60 °C) for 24 h. After removal of excess thionyl chloride by centrifugation, the sample was mixed with 300 mg diamine-terminated PEG ($M_w$ = 1500) and stirred at 100 °C for 24 h under nitrogen protection. Next, this reaction mixture was cooled to ambient temperature and extracted repeatedly with water. The soluble fraction of MWCNTs was separated from the insoluble residue by centrifuging at 1500 rpm for 15 min, and the excess free PEG was removed by repeated filtration with cellulose membrane (pore size = 0.22 $\mu$m). The obtained P-MWCNTs were stored in deionized water [16].

In order to prepare NP-MWCNTs, the acid-treated MWCNTs underwent thermal treatment at 800 °C for 4 h under a nitrogen atmosphere for detaching the functional groups.

TEM (JEM 200CX, Japan), thermogravimetric analysis (TGA, SDT 2900, USA), inductively coupled plasma mass spectrometry (ICP-MS, Leeman Labs, USA), and surface zeta-potential analysis (ZetaSizer 3000HSA, UK) were used to characterize P-MWCNT and NP-MWCNT samples. TEM was also carried out to investigate the state of P-MWCNTs and NP-MWCNTs in the biological environment. In brief, 100 $\mu$l P-MWCNTs or NP-MWCNTs were mixed with 400 $\mu$l serum, and after incubating for 30 min the mixture was dropped on the copper grid for TEM observation.

### *2.3. Animals and treatment*

P-MWCNTs were dispersed in PBS at two concentrations of 0.4 and 2.4 mg ml$^{-1}$ and sterilized under ultraviolet lamplight for 2 h before animal experiments. Also, at the concentrations of 0.4 and 2.4 mg ml$^{-1}$, NP-MWCNTs were dispersed in PBS including 1% (wt%) Tween-80 and sterilized under ultraviolet lamplight for 2 h for the next animal experiments.

One hundred male Kunming mice (22–25 g), 5 weeks old, were obtained from the Second Military Medical University (Shanghai, China) and housed in polycarbonate cages under a 12 h light/dark cycle, and fed with a commercial diet and water *ad libitum*. The pelleted diet was purchased from Shilin Biologic Science and Technology Company (Shanghai, China) and mainly contained dehulled soybean meal, ground corn, ground wheat, wheat middling, soybean oil, fish meal, ground oats, wheat germ, brewers' dried yeast, ground soybean

hulls, several types of vitamin, amino acids and other trace metal elements. The drinking water was tap water. All animal experiments were performed in compliance with the regulations and guidelines of the institutional ethics committee on animal welfare.

Kunming mice were randomly allocated into five groups with 20 mice in each group: PBS group, P-MWCNT groups (10 and 60 mg $kg^{-1}$), and NP-MWCNT groups (10 and 60 mg $kg^{-1}$). Before injection, PBS, the P-MWCNT and NP-MWCNT solutions were sterilized. 300 $\mu$l PBS or MWCNT solution was injected twice into each mouse at the tail vein. After injection, behavior and abnormal symptoms of the mice were monitored.

Ten mice in each group were sacrificed at 15 and 60 days post-administration. The anticoagulant blood samples were collected from the vena ophthalmica with addition of heparin and were centrifuged at 1000 $\times$ g for 10 min. The plasma was harvested and detected immediately or stored at $-20\,^{\circ}$C.

The liver index was calculated as the liver weight (in grams)/body weight (in grams). A piece of liver tissue was stripped and immediately fixed in a 4% formaldehyde or 2.5% glutaraldehyde solution for further histopathological diagnosis and whole genome expression assay. Another piece of liver tissue was stored in liquid nitrogen for the genome expression assay detection. The rest of the liver was immersed in cold saline and then blotted dry, weighed quickly and homogenized in ice cold preparation buffer (including 1 mM Tris(hydroxymethyl) aminomethane hydrochloride, 0.1 mM ethylene diamine tetraacetic acid disodium salt, 0.8% sodium chloride, pH = 7.4) to yield 10% (W/V) homogenate. The homogenates were centrifuged at 2000 r $min^{-1}$ for 8 min at 4 °C and supernatants were used immediately to measure the activity of reduced GSH and SOD or stored at $-80\,^{\circ}$C until assay.

### *2.4. Activity level of GSH and SOD in liver*

The GSH and SOD produced in liver tissues were examined in order to investigate the potential role of oxidative stress. The concentration of GSH in the supernatant was determined by using spectrophotometric diagnostic kits based on Jellow's method [17], using 5,5-dithio-bis-2-nitrobenzoic acid for color development. The yellow color was monitored at 412 nm on a spectrophotometer. The GSH concentration was expressed as mg $g^{-1}$ protein.

Total SOD activity was determined by using spectrophotometric diagnostic kits at 525 nm based on the methods of Beauchamp and Fridovich [18], in which the ratio of auto-oxidation rates of the samples with or without hepatic homogenate was determined. The SOD activity was calculated in terms of units defined as the amount of SOD inhibiting the reduction of nitroblue tetrazolium by 50%.

### *2.5. Histopathological examination of liver tissue*

The liver tissues were fixed with 10% formalin, embedded in paraffin, and stained with hematoxylin–eosin. After routine processing, paraffin sections were cut into 5 $\mu$m thickness and stained with hematoxylin–eosin. Evaluation was performed under a light microscope. The structural changes of cells and tissues were observed.

### *2.6. Electron microscopic study of liver tissue*

Liver tissues were first sliced into 1 mm $\times$ 1 mm $\times$ 1 mm sections and fixed with 2.5% glutaraldehyde in PBS. Then these specimens were post-fixed in 1% osmium tetroxide, dehydrated in a graded alcohol series, and embedded in epoxy resin. After peroxide induced polymerization, these specimens were cut with an ultramicrotome to a thickness of about 50 nm. Finally, the ultrathin liver sections were post-stained with uranyl acetate and lead citrate, and inspected with a Philips electron microscope (model CM-120, Holland).

### *2.7. Whole genome expression array and real-time PCR analysis in liver*

A whole mouse genome microarray was obtained from Phalanx Biotech Group. The whole mouse genome microarray contained 29 922 mouse genome probes, and 1880 experimental control probes, 31 802 probes in all, and they were highly sensitive 70-mer sense-strand polynucleotide probes. The probe set was an abridged version of the mouse exonic evidence based oligonucleotide (MEEBO) probe set developed at Stanford University and the University of California, San Francisco. Each probe was spotted onto the array in a highly consistent manner using an innovative non-contact spotting technology adapted and perfected by Phalanx Biotech for microarray manufacturing.

After the mice was exposed to PBS, P-MWCNTs (60 mg $kg^{-1}$) or NP-MWCNTs (60 mg $kg^{-1}$) for 60 days, the total ribonucleic acid (RNA) of mouse liver was extracted with TRIZOL reagent (Invitrogen). The optical density of RNA was measured by NanoDrop ND-1000. The OD260/280 between 1.93 and 1.99 and OD 260/230 $>$ 2 of all samples were indicative of pure samples without contaminations of organic or carbohydrate origin. Agarose gel electrophoresis was also employed for quality detection. We should see two clear electrophoresis bands at 18S and 28S. The two bands should be fairly sharp and intense. The intensity of the upper band should be about twice that of the lower band. It is normal to see a diffuse smear of ethidium bromide staining material migrating between the 18S and 28S ribosomal bands, probably comprising mRNA and other heterogeneous RNA species.

Double-stranded complementary deoxyribonucleic acids (cDNAs) were synthesized by reverse transcription, and as a template, aRNA was transcribe synthesized rapidly *in vitro* (Ambion MessageAMP aRNA kit). Then aRNA was purified by Qiagen purification column and was fluorescence labeled. The efficiency of fluorescence labeling was detected by a spectrophotometer (ND-1000, Nanodrop, USA) to ensure the reliability of experimental results. The hybridization mix consisted of a 120 $\mu$l 1.5$\times$ one array hybridization buffer and 60 $\mu$l labeled target preparation plus nuclease-free $dH_2O$ hybridized at 50 °C for at least 10 min. Non-specific binding targets were washed away by three different washing steps, and the slides were dried and scanned using GenePix 4000B. The result was automatically digitized for analysis.

**Table 1.** cDNA target genes and primers used for quantitative real-time PCR.

| Gene | Forward primer(5′–3′) Reverse primer(5′-3′) | Length of the products (bp) |
|---|---|---|
| Gsk3b | F: 5′GACTCCTTTACCCTCATTACCTG3′ R: 5′TCTAGCATCAACTCATTTCGG3′ | 180 |
| Gab1 | F: 5′GAAGCAGCCCGATGAATAAAC3′ R: 5′CACCACAACGTAATCCACCCT3′ | 152 |
| Bag4 | F: 5′CAGCGTCCATCAGTATGAATCT3′ R: 5′GCCAATACGCTTTGTCTGTCT3′ | 284 |

A dilution series of DNA template were prepared for standard curves and an appropriate cDNA template was chosen for the PCR reaction. GSk3b, Gab1 and Bag4 primers were all designed using Primer 5.0. Primer sequences and source sequence accession numbers are provided in table 1. A 25 $\mu$l real-time PCR reaction system contained 10 $\mu$M primer F, 10 $\mu$M primer R, 2.5 $\mu$l dNTP (2.5 mM each of dATP, dGTP, dCTP and dTTP), 2.5 $\mu$l 10× PCR buffer (Promega), 1.5 $\mu$l $MgCl_2$ solution (Promega), 1 unit Taq polymerase (Promega), 1 $\mu$l cDNA template and added $dH_2O$ to 25 $\mu$l.

The standard curve sample and the cDNA sample were added into the real-time PCR reaction system [10 $\mu$M primer F, 10 $\mu$M primer R, 0.25× SYBR green (Invitrogen), 2.5 $\mu$l dNTP (2.5 mM each), 2.5 $\mu$l 10× PCR buffer, 1.5 $\mu$l MgCl $_2$ solution, 1 unit Taq polymerase, 1 $\mu$l cDNA template and added $dH_2O$ to 25 $\mu$l], respectively, and then real-time PCR amplification began under the following thermal cycle conditions, 5 min at 95 °C, followed by 35 replicates of 10 s at 95 °C, then 15 s at 59 °C, 20 s at 72 °C, fluorescence detection at 77–85 °C for 5 s. To establish the dissolution curves, the PCR products were slowly heated from 72 to 99 °C.

For each sample, we performed real-time PCR for the target gene and housekeeping gene. The concentration of each gene is generated directly by Rotor-Gene Real-Time Analysis Software 6.0 (Build 14), depending on the standard curve. The relative quantification of the target gene is determined by calculating the ratio between the concentration of the target gene and that of the housekeeping gene.

### 2.8. Biochemical enzymes and TNF-α assay in blood

The biochemical indices, AST, ALT, TB, and Cr, were measured using a biochemical autoanalyzer (Hitachi 7170). TNF-$\alpha$ levels were determined by enzyme linked immunosorbent assay with a commercial kit (catalog number 559732, BD Biosciences, USA), which was used following the manufacturer's instructions.

### 2.9. Statistical analysis

The SPSS software package (SAS Institute Inc., Cary, NC, USA) was used for the analysis of variances. $P < 0.05$ was considered statistically significant. Data were represented as the mean ± SD.

**Table 2.** Physicochemical properties of NP-MWCNT and P-MWCNT samples.

| | Method | P-MWCNTs | NP-MWCNTs |
|---|---|---|---|
| Length ($\mu$m) | TEM | <1 | <1 |
| Diameter (nm) | TEM | 10–20 | 10–20 |
| Surface potential (mV) | Zeta-potential | −1.2 | −2.3 |
| Ni (wt%) | ICP-MS | 0.046 | 0.043 |
| Fe (wt%) | ICP-MS | 0.005 | 0.0064 |
| Zn (wt%) | ICP-MS | 0.0078 | 0.0089 |

## 3. Results

### 3.1. Characterization of P-MWCNTs and NP-MWCNTs

TEM, TGA, and ICP-MS were used to characterize the P-MWCNT and NP-MWCNT samples. TEM investigation shows that both of the MWCNT samples are clean and no bundling, graphite, amorphous carbon, or metal particles are observed. Surface zeta-potential analysis demonstrates that P-MWCNTs and NP-MWCNTs are nearly neutrally charged, but slightly negative. ICP-MS analysis shows that the samples contain small amounts of elemental impurities, mainly Ni, Fe, and Zn, as shown in table 2. The length of P-MWCNTs and NP-MWCNTs is less than 1 $\mu$m in the majority of cases. The TGA result for P-MWCNTs shows that about 23% PEG (w/w) was conjugated with MWCNTs (figure 1). The morphology and length of NP-MWCNTs are similar to those of the P-MWCNTs under the TEM observation. P-MWCNTs and NP-MWCNTs do not aggregate to form big aggregations in mouse serum (figure 2).

### 3.2. General toxicity

Mice did not show differences in vocalizations, labored breathing, difficulty in moving, hunching, or interactions with cage mates in any group, except that those mice in the 60 mg MWCT group appeared sluggish and congregated at the corner of the cage on day 1 after injection. There was no significant difference among all groups on the body weight change and liver index of mice ($P > 0.05$, figure 3). The photos of mouse liver exposed to P-MWCNTs or NP-MWCNTs are shown in figure 4; the liver color gradually turns to black as the injection dose increases, indicating that more P-MWCNTs or NP-MWCNTs were trapped in the mouse liver.

### 3.3. Histopathological examination and electron microscopic study

Figure 5 shows the histological changes in mouse liver in all groups after treatment. There is no obvious damage observed in the liver at the dose of 10 mg $kg^{-1}$. However, there is severe inflammatory cell infiltration in the portal region, cellular necrosis and focal necrosis at the dose of 60 mg $kg^{-1}$ in the NP-MWCNT group, but in the P-MWCNT group there is only slight inflammatory cell infiltration at 60 days post-exposure. The results demonstrate that the liver damage in

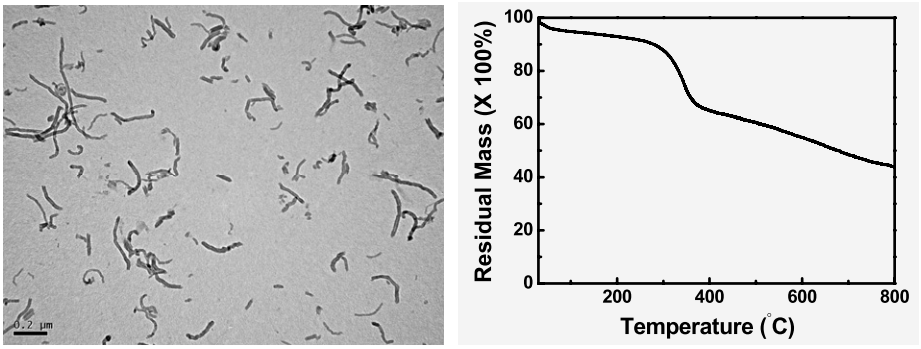


**Figure 1.** TEM image and TGA curve of P-MWCNTs.

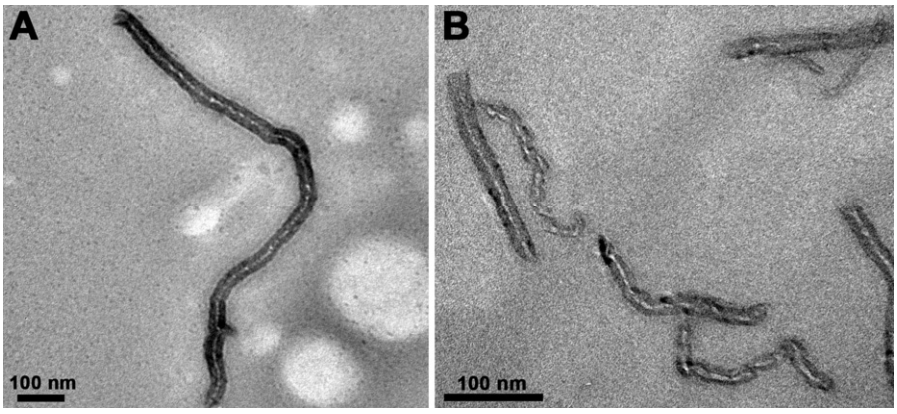


**Figure 2.** TEM images of P-MWCNTs (A) and NP-MWCNTs (B) in mouse serum.

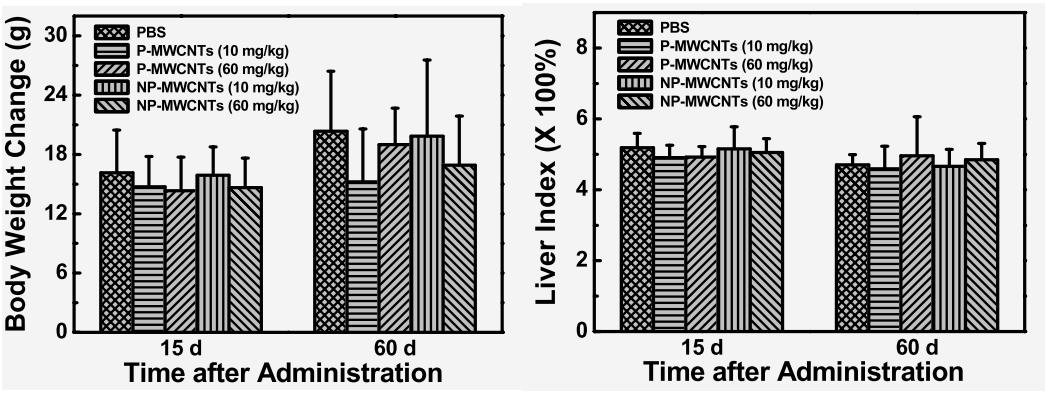


**Figure 3.** Body weight change (left) and liver index (right) of mice exposed intravenously to different doses of P-MWCNTs or NP-MWCNTs at 15 or 60 days post-exposure. Data are presented as the mean ± SD $n = 10$; $^{*}P < 0.05$ is considered statistically significant compared with the PBS group.

the NP-MWCNT group is more severe than in the P-MWCNT group.

In order to further investigate the liver damage by NP-MWCNTs and P-MWCNTs, electron microscopic observation was carried out. Figure 6 shows typical electron micrographs of liver exposed to 60 mg $kg^{-1}$ of P-MWCNTs or NP-MWCNTs at 15 or 60 days post-exposure. The images show that NP-MWCNTs would induce mitochondrial destruction and lysis at 60 days, whereas P-MWCNTs only induce slight mitochondrial swelling. The liver of the P-MWCNT and NP-MWCNT group at 15 days is not significantly different from that of the PBS group. On the whole, the NP-MWCNT group exhibits more severe histological changes in comparison with the P-MWCNT group.

### *3.4. Oxidative stress damage in liver*

Oxidative stress is an imbalance between the production of reactive oxygen species (ROS) and their degradation by antioxidants. ROS interact uncontrollably with the cell

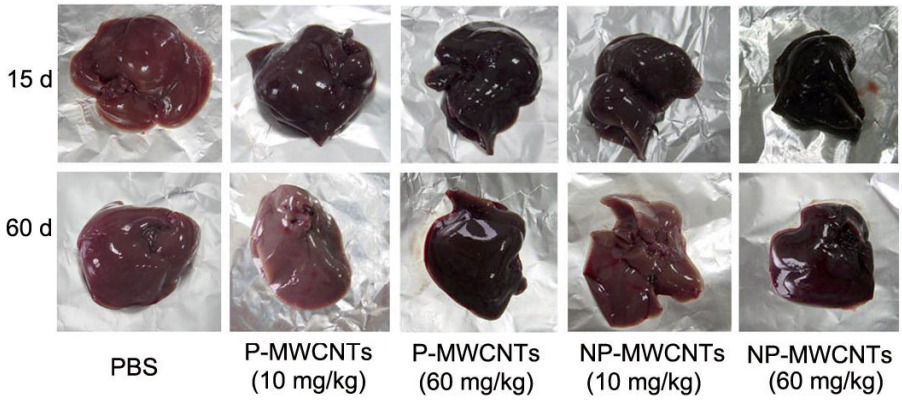


**Figure 4.** Photos of mouse liver exposed to different doses of P-MWCNTs or NP-MWCNTs at 15 or 60 days post-exposure.

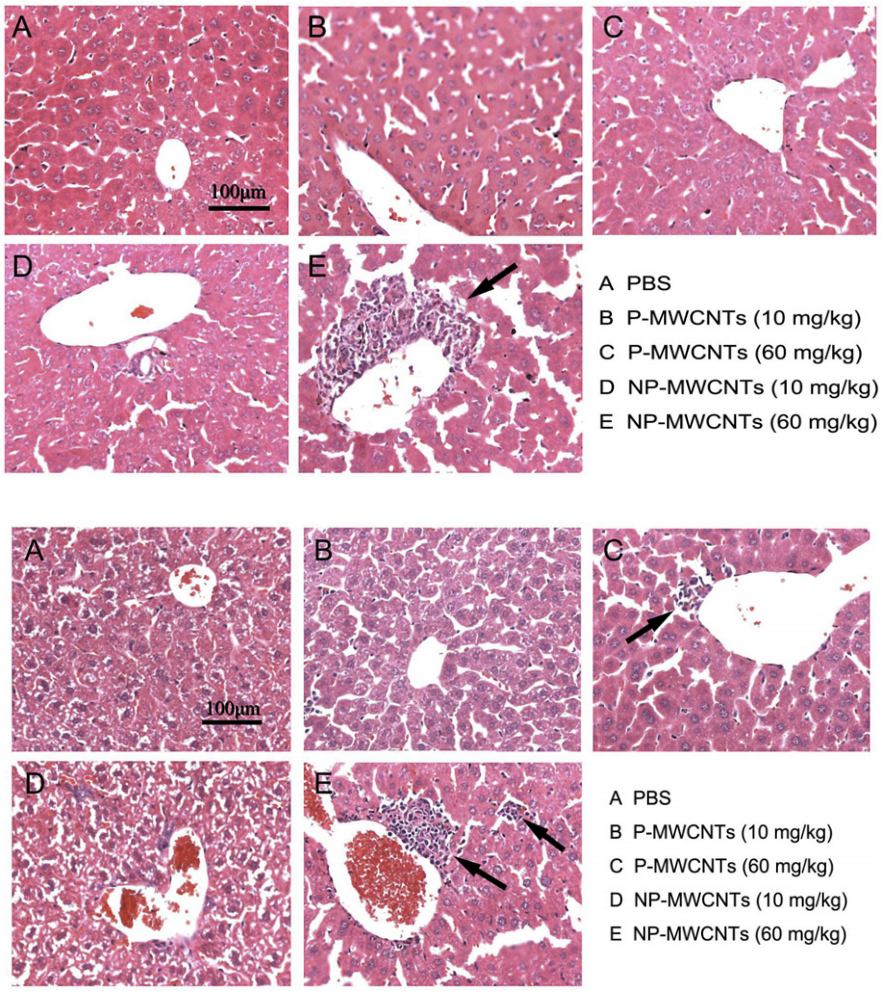


**Figure 5.** Histological morphological change of mouse liver exposed to different doses of P-MWCNTs or NP-MWCNTs at 15 (top) and 60 (bottom) days post-exposure. The black arrows indicate inflammatory infiltrate and low-grade spotty necrosis.

membrane, DNA or other cell compounds, thereby severely damaging these cell constituents [19]. GSH and SOD are two important antioxidant enzymes for balancing the ROS level. Figure 7 shows the GSH level and SOD activity in mouse liver at 15 and 60 days after injection of different doses of P-MWCNTs or NP-MWCNTs. The results indicate that there is no significant difference among all five groups.

### *3.5. Whole genome expression array in liver*

The results of whole genome expression show that there are changes in the genes in MWCNT-exposed groups compared with the PBS group. These genes include those for the antigen processing and presentation pathway, cholesterol biosynthesis, the IL-6 signaling pathway, the TNF-$\alpha$ and nuclear factor

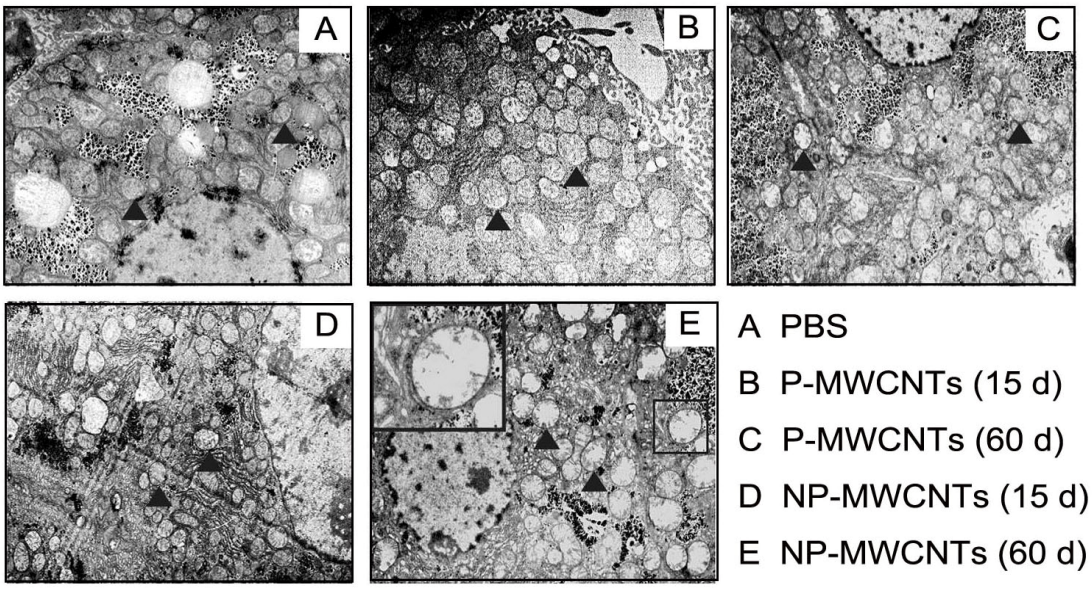


**Figure 6.** Electron micrographic change of liver in mouse exposed to 60 mg $kg^{-1}$ P-MWCNTs ((B) and (C)) or NP-MWCNTs ((D) and (E)) at 15 or 60 days post-exposure. Mitochondria are indicated by arrows. In (E) the inset picture is the zoom of the small black rectangle and obviously exhibits mitochondrial destruction, loss and lysis of the mitochondrial crest.

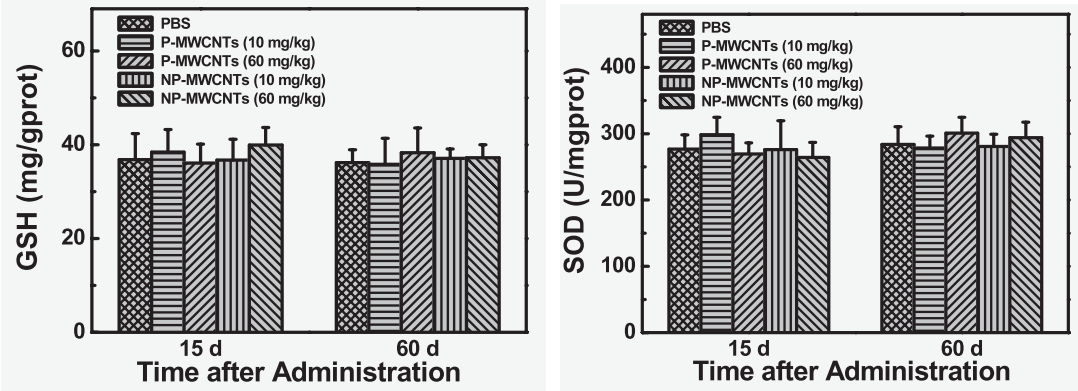


**Figure 7.** Changes of GSH level and SOD activity in mouse liver exposed to different doses of P-MWCNTs or NP-MWCNTs at 15 or 60 days post-exposure. Data are presented as the mean ± SD $n = 10$; $^{*}P < 0.05$ is considered statistically significant compared with the PBS group.

kappa B (NF-$\kappa$B) signaling pathway, the cell cycle and metabolism of xenobiotics by cytochrome P450, etc. The regulatory function of Gsk3b, Bag4, and Gab1 in TNF-$\alpha$ and NF-$\kappa$B signaling pathways is obvious. Thus we choose this pathway to carry out the real-time polymerase chain reaction experiment. The expression of Bag4 and Gab1 increases in mouse liver in 60 mg $kg^{-1}$ NP-MWCNT or P-MWCNT groups compared with PBS group ($P < 0.05$). However, there is no significant difference between the P-MWCNT and NP-MWCNT group. The P-MWCNTs down-regulates Gsk3b expression ($P < 0.05$), whilst the NP-MWCNTs do not influence Gsk3b expression ($P > 0.05$) (figure 8).

### *3.6. Biochemical enzymes and TNF-α in blood*

Figure 9 shows the concentration of AST, ALT, Cr, and TB in mouse blood of each group at 15 and 60 days post-exposure. The AST concentration in the NP-MWCNT group is higher than that in the PBS group, and gradually increases with increasing injection dose of NP-MWCNTs at 15 days post-exposure ($P < 0.05$). At 60 days it is higher only in the NP-MWCNT group (60 mg $kg^{-1}$) than in PBS group. However, the AST concentration in the P-MWCNT group is not significantly different from that of PBS group through the entire period. As for ALT and Cr, there is no difference among five groups at 15 and 60 days post-exposure ($P > 0.05$). The TB concentration in NP-MWCNT or P-MWCNT groups increases, but not significantly, compared with that in the PBS group ($P > 0.05$).

TNF-$\alpha$ is considered as one of the most important promoters of inflammation, necrosis and fibrosis in liver damage [20]. Figure 10 shows the TNF-$\alpha$ concentration in plasma of mice at different exposed doses and intervals. There is no significant difference among all five groups. This means that the NP-MWCNTs and P-MWCNTs do not induce an inflammatory response in mice.

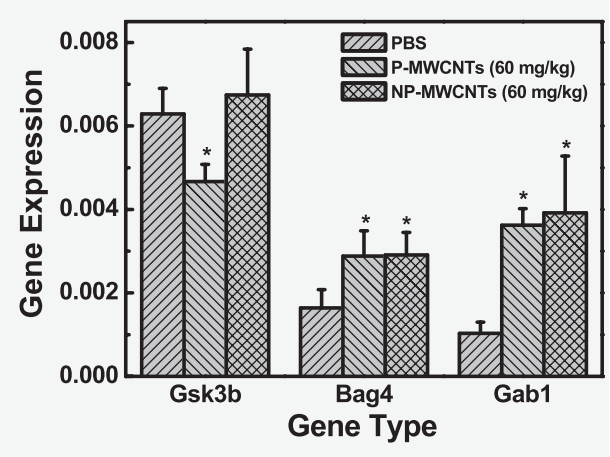


**Figure 8.** After mice were exposed to 60 mg $kg^{-1}$ P-MWCNTs or NP-MWCNTs for 60 days, three genes in the TNF-$\alpha$ and NF-$\kappa$B signaling pathway of mouse liver change compared with exposure to PBS. Data are presented as the mean $\pm$ SD $n = 3$; $^{*}P < 0.05$ is considered statistically significant compared with the PBS group.

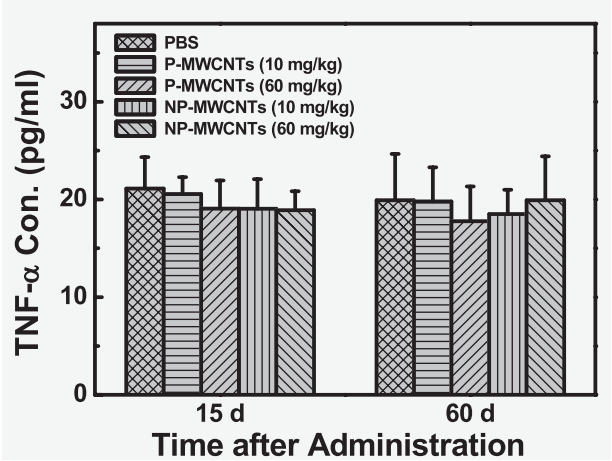


**Figure 10.** TNF-$\alpha$ concentration in blood of mice exposed to P-MWCNTs or NP-MWCNTs at different doses and intervals. Data are presented as the mean $\pm$ SD $n = 5$; $^{*}P < 0.05$ is considered statistically significant compared with the PBS group.

## 4. Discussion

The liver is the largest detoxifying tissue and the major target organ where *in vivo* CNTs are entrapped [21, 22]. Drugs and nutrients will not be efficiently absorbed by organisms when the liver is injured. In this paper, liver was selected for investigating the potential toxicity of P-MWCNTs *in vivo*. As the control, a toxicity assay of PBS and NP-MWCNTs was also carried out. Following our previous findings [21, 23], a low (10 mg $kg^{-1}$) and high dosage (60 mg $kg^{-1}$) were intravenously injected into mice. The black

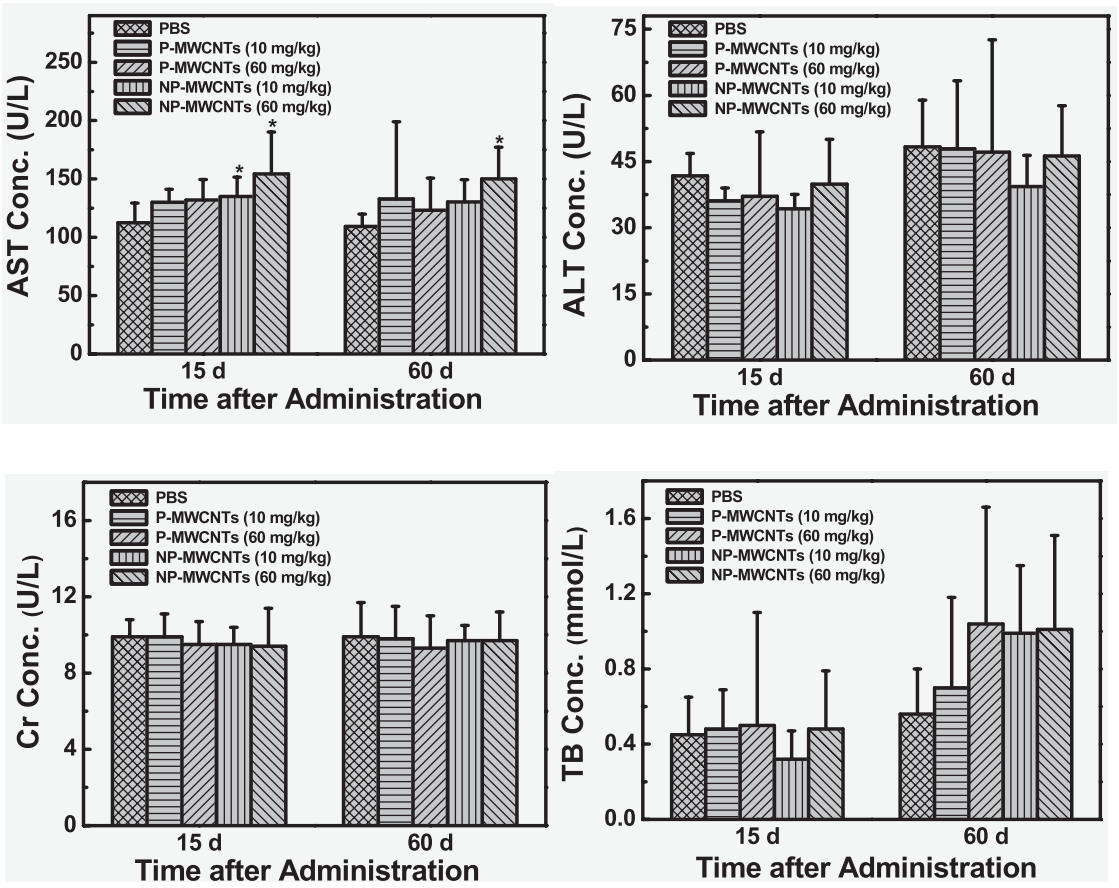


**Figure 9.** AST, ALT, Cr, or TB concentration in blood of mice exposed to P-MWCNTs or NP-MWCNTs at different doses and different time intervals. Data are presented as the mean $\pm$ SD $n = 5$; $^{*}P < 0.05$ is considered statistically significant compared with the PBS group.

color of liver indicates pronounced deposition of MWCNTs, and the deposition enhances with increasing injection dose of MWCNTs. The liver color of the P-MWCNT group seems lighter than that of the NP-MWCNT group at the same dosage and post-exposure interval. This is consistent with the results of Liu *et al*, who suggest that PEGylated SWCNTs are slowly excreted from the body following systemic distribution in the mouse model [14].

AST, ALT, Cr, and TB are important biochemical enzymes reflecting hepatic injury [24]. Liver damage increases the levels of AST, ALT, Cr, and TB. The results show that the blood concentration of AST in some NP-MWCNT groups significantly increases compared with that of the PBS group. However, there is no similar observed increase in the P-MWCNT groups. This implies that P-MWNCT is less toxic (induces less hepatic injury). The concentration of TB in NP-MWCNT and MWCNT group is higher than that of PBS group at 60 days, but the difference is not statistically significant ($P > 0.05$). Hepatocyte injury can induce dysfunction of uptake, combination and excretion of bilirubin. We suggest that NP-MWCNTs and P-MWCNTs may cause slight, but not severe, liver inflammation.

The histological examination and electron microscopic study confirmed that NP-MWCNTs induced slightly more severe damage in liver than P-MWCNTs did. The histological images show the high dose of NP-MWCNTs induces a hepatic inflammatory response and spot necrosis, whereas P-MWCNTs induce a slight hepatic inflammatory response. And the electron micrographs also demonstrate that NP-MWCNTs induce mitochondrial destruction and lysis of mouse liver at 60 days post-exposure. In fact, many previous studies have shown that the surface functionalization plays an important role in the variation in toxicology of CNTs. Sayes *et al* have shown a decreased cytotoxicity with an increased functionality of SWCNTs using human dermal fibroblasts [25]. Cheng *et al* also showed that well purified and modified MWCNTs did not have serious toxic impacts in loaded zebrafish, which suggested that intensive purification and functionalization processes could help improve the biocompatibility of CNTs in biological systems [26].

Since the oxidative stress model has been proposed to predict the toxicity of engineered nanoparticles [21], more and more studies have paid attention to the oxidative damage of nanomaterials *in vitro* and *in vivo*. However, to date, this oxidative stress model for CNTs is a matter of debate. Sarkar *et al* reported that SWCNTs induced oxidative stress and indicated the activation of a specific signaling pathway in keratinocytes [27]. But most of the other related work has shown the metal impurities played an important role in the ROS process [28]. *In vitro* studies with NR8383 and A549 cells suggested that pristine CNT exposure induced cellular oxidative stress. However, when the CNTs were acid treated to remove metal contaminants, cellular ROS generation did not occur, suggesting the metal catalyst contaminants were responsible for the generation of ROS [29]. In the present study, the purity of P-MWCNTs and NP-MWCNTs is very high and the samples only contain tiny amounts of metal impurities. Also, there is no observed oxidative stress caused by MWCNTs and P-MWCNTs, and this again supports that high purity CNTs do not induce oxidative stress.

TNF-$\alpha$ is a multifunctional proinflammatory cytokine that belongs to the tumor necrosis factor superfamily. NF-$\kappa$B is a transcription regulator that is activated by various intra- and extra-cellular stimuli including cytokines like TNF-$\alpha$ [30]. This pathway is involved in the regulation of a wide spectrum of biological processes including cell proliferation, differentiation, apoptosis, lipid metabolism, and coagulation. There are three types of gene in the TNF-$\alpha$ and NF-$\kappa$B signaling pathway, including Gsk3b, Bag4, and Gab1. Gsk3b is a proline-directed serine–threonine kinase and participates in the TNF-$\alpha$ signaling pathway and regulates cellular metabolism and the cell cycle [31]. Our result showed that the P-MWCNT group mice down-regulate Gsk3b expression ($P < 0.05$) and this may infer that P-MWCNTs reduce the inflammatory reaction. Bag4 is a member of the Bag1-related protein family. This protein was found to be associated with the death domain of TNF receptor type 1 and death receptor-3, and thereby negatively regulates downstream cell death signaling. Gab1 is a component in oxidative stress signaling and has a dual role in cell survival: it plays a central role in regulating hepatocyte growth factor synergy but also in its action on Hep3B cell growth inhibition [32]. Our present study shows that both P-MWCNTs and NP-MWCNTs can up-regulate Bag4 and Gab1 gene expression, and there is no significant difference between the two groups. Thus, both P-MWCNTs and NP-MWCNTs can regulate gene expression in liver in the TNF-$\alpha$ signaling pathway. This result means that they partly induce liver inflammation, and is consistent with the histopathological examination and electron microscopic imaging. In order to further reveal whether the P-MWCNTs and NP-MWCNT will induce hepatic damage *in vivo*, more tests on gene expression are needed.

## 5. Conclusions

We have intensively investigated and compared the *in vivo* toxicity of P-MWCNTs and NP-MWCNTs throughout a 2 month period. Both P-MWCNTs and NP-MWCNTs can induce gene expression changes in liver, especially in the TNF-$\alpha$ and NF-$\kappa$B signaling pathway. However, there was no significant oxidative stress damage in mouse liver among all groups. Furthermore, the histological images and electron micrographs show that both P-MWCNTs and NP-MWCNTs induce hepatic inflammatory response, spot necrosis and mitochondrial destruction. However, these results also demonstrate that NP-MWCNTs show a slightly higher *in vivo* toxicity than P-MWCNTs, and PEGylation could partly, but not considerably, improve the biocompatibility of MWCNTs *in vivo*. These findings have provided some basic information on the biocompatibility of P-MWCNTs which is beneficial for their future biomedical applications.

## Acknowledgments

The research was funded by the China Ministry of Science and Technology (2006CB705604, 2007CB936000), China Natural

Science Foundation (40830744, 20907028), China Ministry of Health (2009ZX10004-301), Science and Technology Commission of Shanghai Municipality (09XD1401800 and 08ZR1407800) and Shanghai Leading Academic Disciplines (S30109).

## References

[1] Lu F, Gu L, Meziani M, Wang X, Luo P, Veca L, Cao L and Sun Y 2009 *Adv. Mater.* **21** 139
[2] Liu Z, Tabakman S, Welsher K and Dai H 2009 *Nano Res.* **2** 85
[3] Liu Z, Sun X, Nakayama N and Dai H J 2007 *ACS Nano* **1** 50
[4] Yang S T *et al* 2008 *Small* **4** 940
[5] Cato M H *et al* 2008 *J. Nanosci. Nanotechnol.* **8** 2259
[6] Ou Z M, Wu B Y, Xing D, Zhou F F, Wang H Y and Tang Y H 2009 *Nanotechnology* **20** 105102
[7] Cheng J P, Fernando K A S, Veca L M, Sun Y P, Lamond A I, Lam Y W and Cheng S H 2008 *ACS Nano* **2** 2085–94
[8] Shvedova A A, Kisin E R, Porter D, Schulte P, Kagan V E, Fadeel B and Castranova V 2009 *Pharmacol. Therapeut.* **121** 192
[9] Poland C A, Duffin R, Kinloch I, Maynard A, Wallace W A H, Seaton A, Stone V, Brown S, MacNee W and Donaldson K 2008 *Nat. Nanotechnol.* **3** 423
[10] Smart S K, Cassady A I, Lu G Q and Martin D J 2006 *Carbon* **44** 1034
[11] Dhar S, Liu Z, Thomale J, Dai H J and Lippard S J 2008 *J. Am. Chem. Soc.* **130** 11467
[12] Kam N W S, O'Connell M, Wisdom J A and Dai H J 2005 *Proc. Natl Acad. Sci. USA* **102** 11600
[13] Liu Z, Winters M, Holodniy M and Dai H J 2007 *Angew. Chem. Int. Edn* **46** 2023
[14] Liu Z, Davis C, Cai W B, He L, Chen X Y and Dai H J 2008 *Proc. Natl Acad. Sci. USA* **105** 1410
[15] Schipper M L, Nakayama-Ratchford N, Davis C R, Kam N M S, Chu P, Liu Z, Sun X M, Dai H J and Gambhir S S 2008 *Nat. Nanotechnol.* **3** 216
[16] Sun Y F, Wu F, Deng X Y, Xiong D M, Zhao B, Wu M H and Jiao Z 2008 *Chin. J. Inorg. Chem.* **24** 98
[17] Jollow D J, Mitchell J R, Zampaglione N and Gillette J R 1974 *Pharmacology* **11** 151
[18] Beauchamp C and Fridovich I 1971 *Anal. Biochem.* **44** 276
[19] Nel A, Xia T, Madler L and Li N 2006 *Science* **311** 622
[20] Fernandez-Martinez E, Perez-Alvarez V, Tsutsumi V, Shibayama M and Muriel P 2006 *Exp. Toxicol. Pathol.* **58** 49
[21] Deng X Y, Jia G, Wang H F, Sun H F, Wang X, Yang S T, Wang T and Liu Y 2007 *Carbon* **45** 1419
[22] Deng X Y, Yang S T, Nie H Y, Wang H F and Liu Y F 2008 *Nanotechnology* **19** 075101
[23] Deng X Y, Wu F, Liu Z, Luo M, Li L, Ni Q S, Jiao Z, Wu M H and Liu Y F 2009 *Carbon* **47** 1421
[24] Murakami S, Okubo K, Tsuji Y, Sakata H, Takahashi T, Kikuchi M and Hirayama R 2004 *World J. Surg.* **28** 671
[25] Sayes C M *et al* 2006 *Toxicol. Lett.* **161** 135
[26] Cheng J P, Chan C M, Veca L M, Poon W L, Chan P K, Qu L W, Sun Y P and Cheng S H 2009 *Toxicol. Appl. Pharm.* **235** 216
[27] Sarkar S, Sharma C, Yog R, Periakaruppan A, Jejelowo O, Thomas R, Barrera E V, Rice-Ficht A C, Wilson B L and Ramesh G T 2007 *J. Nanosci. Nanotechnol.* **7** 584
[28] Shvedova A A, Kisin E R, Mercer R, Murray A R, Johnson V J, Potapovick A I, Tyurina Y Y, Gorelik O, Arepalli S and Schwegler-Berry D 2005 *Am. J. Physiol. Lung Cell Mol. Physiol.* **289** 698
[29] Pulskamp K, Diabate S and Krug H F 2007 *Toxicol. Lett.* **168** 58
[30] Di Giuseppe M, Gambelli F, Hoyle G W, Lungarella G, Studer S M, Richards T, Yousem S, McCurry K, Dauber J and Kaminski N 2009 *PLoS ONE* **4** e5689
[31] Seiden-Long I, Navab R, Shih W, Li M, Chow J, Zhu C Q, Radulovich N, Saucier C and Tsao M S 2008 *Carcinogenesis* **29** 647
[32] Wang Z, Ge L, Wang M and Carr B I 2007 *Hepatology* **46** 2003